Lecture 15: Detecting Objects by Parts

David R. Morales, Austin O. Narcomey, Minh-An Quinn, Guilherme Reis, Omar Solis
Department of Computer Science
Stanford University
Stanford, CA 94305
{mrlsdvd, aon2, minhan, greis, osolis9}@stanford.edu

1 Introduction to Object Detection

Previously, we introduced methods for detecting objects in an image; in this lecture, we describe methods that detect and localize generic objects in images from various categories such as cars and people. The categories that are detected depend on the application domain. For example, self-driving cars need to detect other cars and traffic signs.

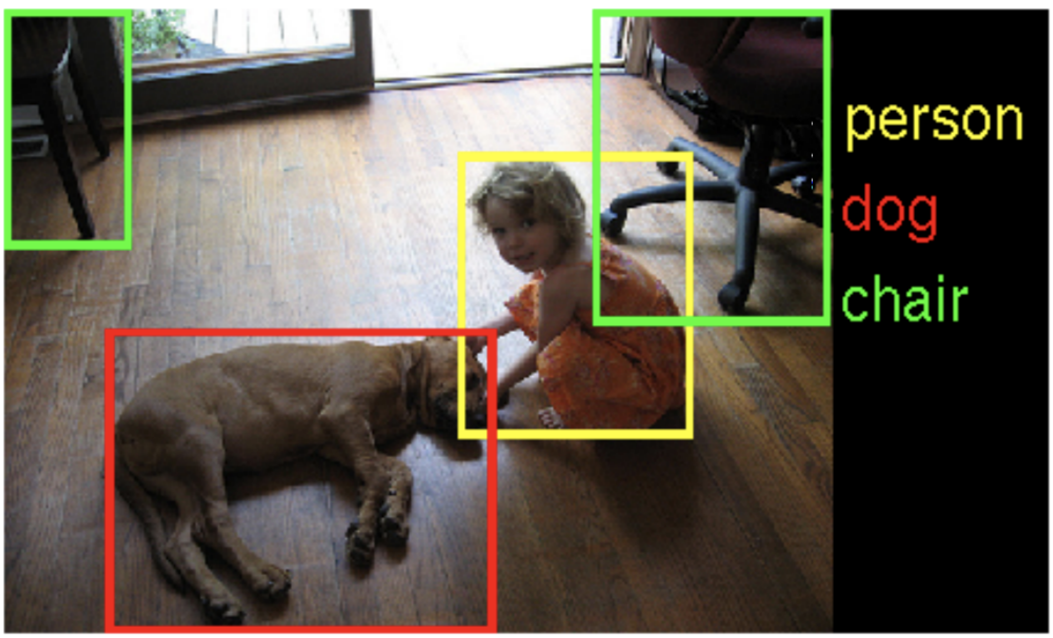

Figure 1: An example of an object detection algorithm detecting the categories of a person, dog, and a chair

1.1 Challenges

Object detection, however, faces many challenges. The challenges include the varying illumination conditions, changes in the viewpoints, object deformations, and intra-class variability; this makes objects of the same category appear different and makes it difficult to correctly detect and classify objects. In addition, the algorithms introduced herein only give the 2D location of the object in the image and not the 3D location. For example, the algorithms cannot determine if an object is in front or behind another object. Additionally, the following object detectors do not provide the boundary of an object it finds; the object detector just provides a bounding box of where the object was found.

2 Current Object Detection Benchmarks

Today, object detection has practically been addressed for certain applications such as face detection. To evaluate the performance of an object detector, researchers use standardized object detection benchmarks. Benchmarks are used to make sure we are moving forward and performing better with new research.

2.1 PASCAL VOC

The first widely used benchmark was the PASCAL VOC Challenge [2], or the Pattern Analysis, Statistical Modeling, and Computational Learning Visual Object Classes challenge. The PASCAL VOC challenge was used from 2005 to 2012 and tested 20 categories. PASCAL was regarded as a high quality benchmark because its test categories had high variability within each category. Each test image also had bounding boxes for all objects of interest like cars, people, cats, etc. PASCAL also had annual classification, detection, and segmentation challenges.

2.2 ImageNet Large Scale Visual Recognition Challenge

The benchmark that replaced PASCAL is the ImageNet Large Scale Visual Recognition Challenge (ILSVR) [5]. The ILSVR Challenge tested 200 categories of objects, significantly more than what PASCAL tested, had more variability in the object types, and had many objects in a single image.

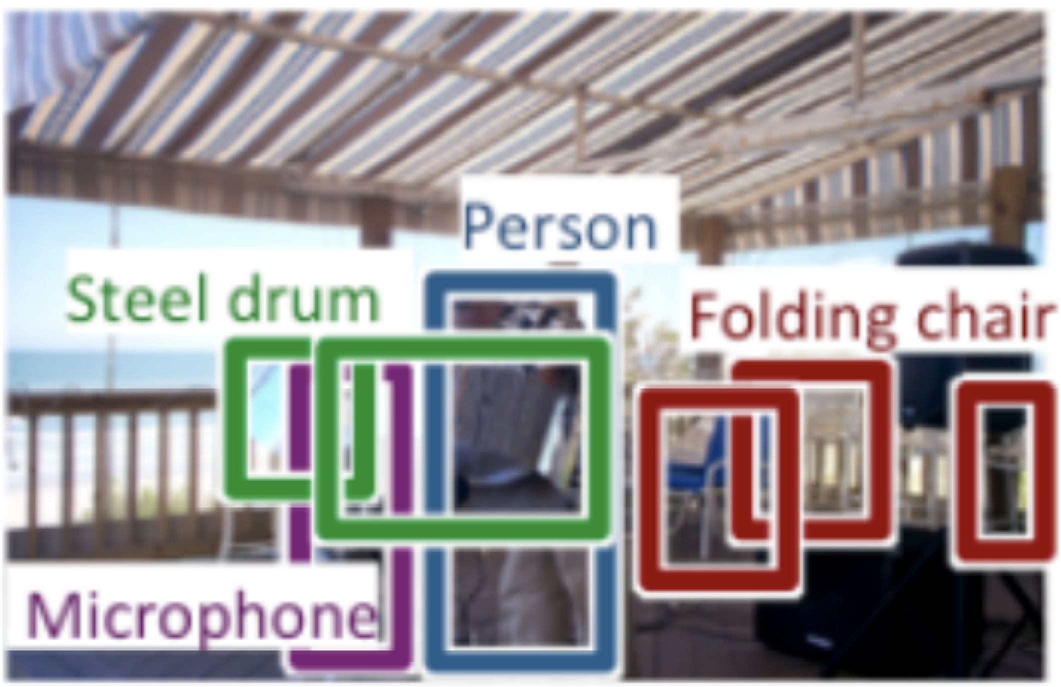

Figure 2: An example of a labeled ILSVR test image.

2.3 Common Objects in Context

Another benchmark that is still used today is the Common Objects in Context (COCO) challenge [3]. The COCO challenge tests 80 categories, but in addition to testing bounding boxes of locations of objects, it also tests object segmentation, which are detailed bounding areas of an object. Creating the test images for the dataset used in the COCO challenge is very time consuming because each object that is tested needs to be traced almost perfectly.

Figure 3: Object segmentation used for the COCO challenge.

3 Evaluating Object Detection

When evaluating an object detection algorithm, we want to compare the predictions with ground truth. The ground truth is provided by humans who manually classify and locate objects in the images.

Figure 4: Yellow boxes represent ground truth while green boxes are predictions.

When comparing predictions with ground truth, there are four different possibilities:

1. True Positive (TP)
True positives are objects that both the algorithm (prediction) and annotator (ground truth) locate. In order to be more robust to slight variations between the prediction and ground truth, predictions are considered true positives when the overlap between the prediction and ground truth is greater than 0.5 (Figure 5a). The overlap between the prediction and ground truth is defined as the intersection over the union of the prediction and ground truth. True positives are also sometimes referred to as hits.

2. False Positive (FP)
False positives are objects that the algorithm (prediction) locates but the annotator (ground truth) does not locate. More formally, false positives occur where the overlap of the prediction and ground truth is less than 0.5 (Figure 5b). False positives are also referred to as false alarms.

3. False Negative (FN)
False negatives are ground truth objects that our model does not find (Figure 5b). These can also be referred to as misses.

4. True Negative (TN)
True negatives are anywhere our algorithm didn't produce a box and the annotator did not provide a box. True negatives are also called correct rejections.

(a) (b) (c)

Figure 5: Example classifications using an overlap threshold of 0.5. (a) True positive, because ground truth (yellow box) and prediction (green box) overlap is more than 0.5. (b) False positive, since the prediction boxes (green) do not overlap with any ground truth boxes. (c) False negative, since the ground truth box (yellow) is not detected by the model.

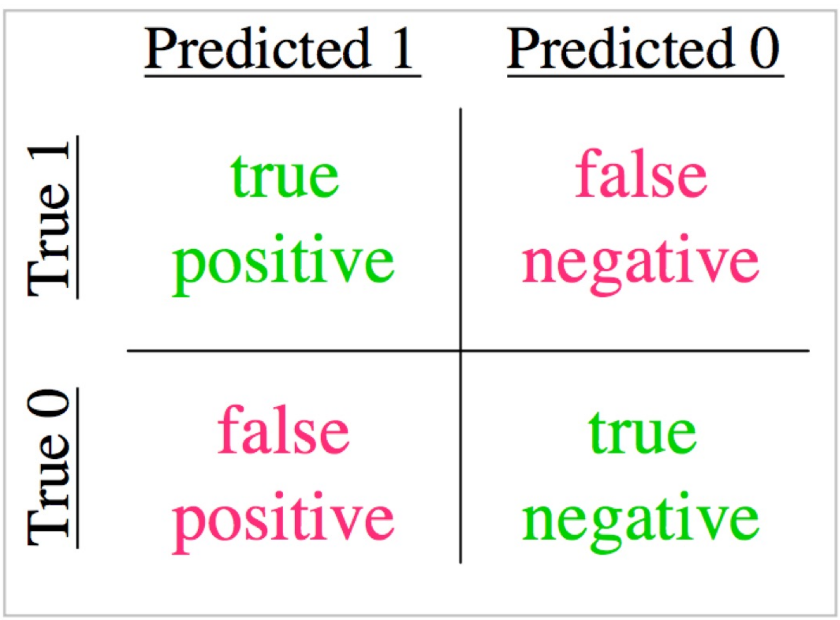

Figure 6: Summary chart of classifications, with green being counts you want to maximize and red being counts you want to minimize.

In general, we want to minimize false positives and false negatives while maximizing true positives and true negatives (Figure 6.

Using the counts of true positives (TP), true negatives (TN), false positives (FP), and false negatives (FN), we can calculate two measures: precision and recall.

$$Precision = \frac{TP}{TP + FP}$$

Precision can be thought of as the fraction of correct object predictions among all objects detected by the model.

$$Recall = \frac{TP}{TP + FN}$$

Recall can be thought of as the fraction of ground truth objects that are correctly detected by the model.

Figure 7: Predictions are green boxes while ground truth is yellow. All the ground truths are correctly predicted, making recall perfect. However, precision is low, since there are many false positives.

For every threshold we use to define true positives (In Figure 5 the overlap threshold was set to 0.5), we can measure the precision and recall. Using that information, we can create a Precision-Recall curve (PR curve). Generally, we want to maximize both precision and recall. Therefore, for a perfect model, precision would be 1 and recall would be 1, for all thresholds. When comparing different models and parameters, we can compare the PR curves. The better models have more area under the curve.

However, depending on the application, we may want specific values for precision and recall. Therefore, you can choose the best model by fixing, say the recall, and finding the model that has the best precision at that recall.

We can also use the counts of TP, FP, TN, and FN to see how our model is making errors.

4 A Simple Sliding Window Detector

The detection can be treated as a classification problem. Instead of attempting to produce the location of objects in an image by processing the entire image at once, slide a window over the image and classify each position of the window as either containing an object or not (Figure 9).

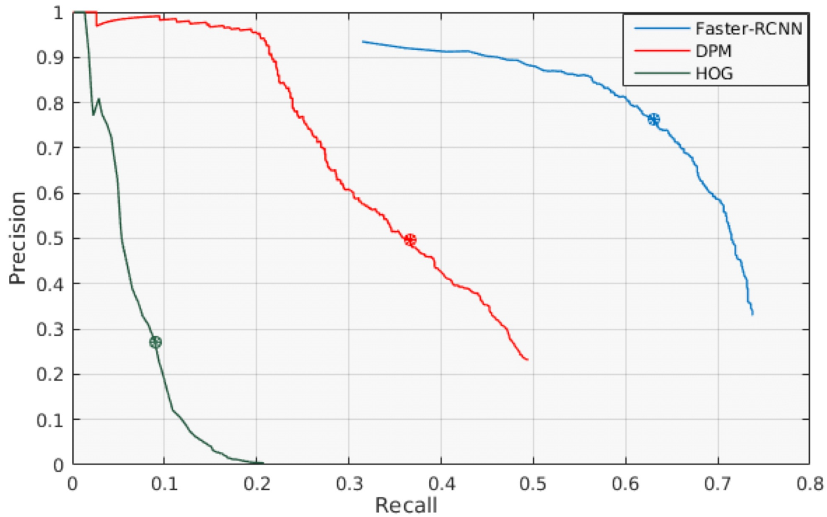

Figure 8: Faster-RCNN model is the best of the three models since it has the most area under the curve.

(a)

(b)

(c)

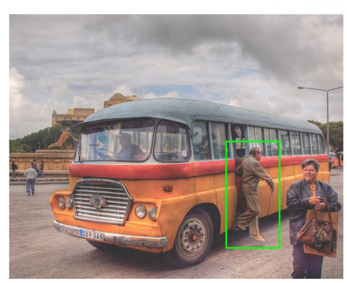

(d)

Figure 9: Consider the problem of detecting people in an image. (a) - (c) sliding window across image and at each position classifying window as not containing a person. (b) window over person and classifying window as containing a person. Image source: Flickr user neilalderney123

4.1 Feature Extraction and Object Representation

Dalal and Triggs [1] showed the effectiveness of using Histograms of Oriented Gradient (HOG) descriptors for human detection. Although their feature extraction methods were focused on human detection, they can be applied for detecting various objects.

Recall HOG descriptors from lecture 8. An image window is divided into blocks; the magnitude of the gradients of the pixels in each block are accumulated into bins according to the direction of the gradients. These local histograms of the blocks are then normalized and concatenated to produce a feature representation of the image window.

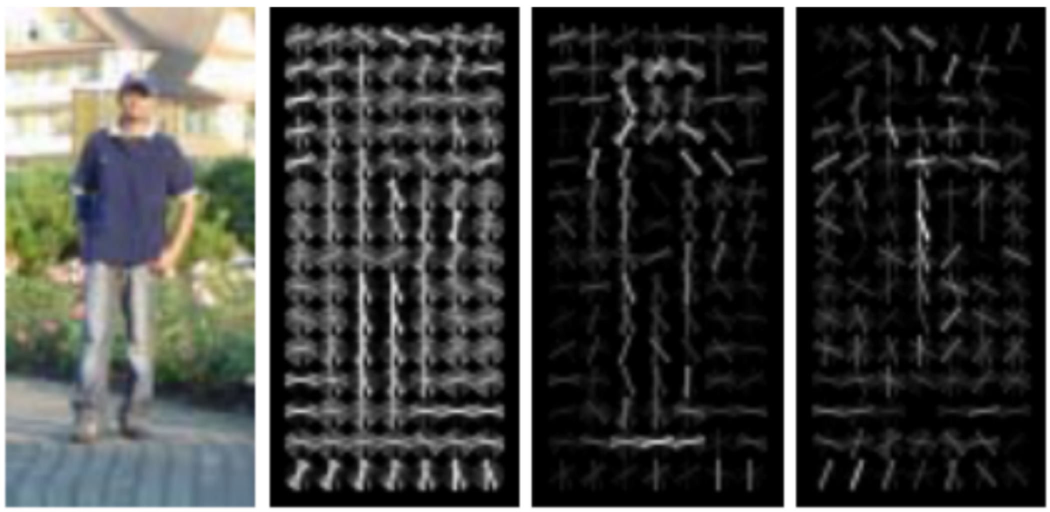

Figure 10: An image of a person along with its respective HOG descriptor. Note that the last two images are the HOG descriptor weighted by the positive and negative weights of the classifier using them. The outline of the person is very visible in the weighted descriptors. Image source: Dalal and Triggs [1]

Figure 10 shows an example of transforming an image into a HOG feature space. Producing a prototypical representation of an object would then involve considering many image windows labeled with containing that object. One approach to creating this representation would be to train a classifier on the HOG descriptors of these many labeled image windows and then proceed to use the trained classifier to classify the windows in images of interest. In their aim to improve human detection, for example, Dalal and Triggs [1] train a linear Support Vector Machine on the HOG descriptors of image windows containing people.

A more simple approach, and the approach that will be assumed below, is that of averaging the window images containing an object of interest and then extracting the HOG descriptor of that average image to create a template for the object (Figure 11).

4.2 Classifying Windows

Now that we have a method for extracting useful features from an image window and for constructing object templates, we can proceed to detecting objects in images. The idea is to compare each window with the object template and search for matches. That is, the object template itself acts as a filter that slides across the image. At each position, the HOG descriptor of the window being compared is extracted and a similarity score between the two HOG descriptors is computed. If the similarity score at some location is above a predefined detection threshold, then an object can be said to have been detected in the window at that location.

The similarity score can be as simple as the dot product of the window HOG descriptor and the template HOG descriptor. This is the scoring method that is assumed in following sections.

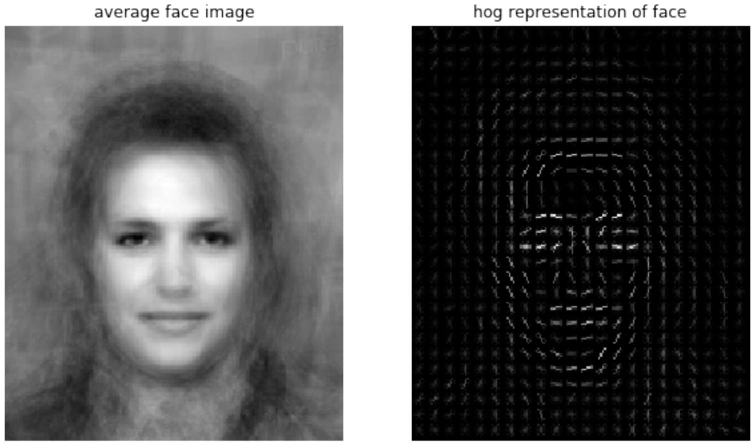

Figure 11: The average face image above is created by averaging 31 aligned face images of the same size. The HOG descriptor of this average face image can then be used as a template for detecting faces in images.

As effective as the method seems so far, it's success is very limited by the size of the sliding template window. For example, consider the case where objects are larger than the template being used to detect them (Figure 12).

(a)

(b)

Figure 12: Consider, again, the problem of detecting people, except this time our sliding window is much smaller. (a) The template and sliding window are still large enough to detect the smaller, distant person. (b) The person in the foreground is a lot bigger than our window size and is not being detected.

4.3 Multi Scale Sliding Window

To account for variations in size of the objects being detected, multiple scalings of the the image are considered. A feature pyramid (Figure 13) of different image resizings is created. The sliding window technique is then applied as usual over all the the pyramid levels. The window that produces the highest similarity score out of the resizings is used as the location of the detected object.

5 The Deformable Parts Model (DPM)

The simple sliding window detector is not robust to small changes in shape (such as a face where the eyebrows are raised or the eyes are further apart, or cars where the wheel's may be farther apart or the car may be longer) so we want a new detection model that can handle these situations. Recall the

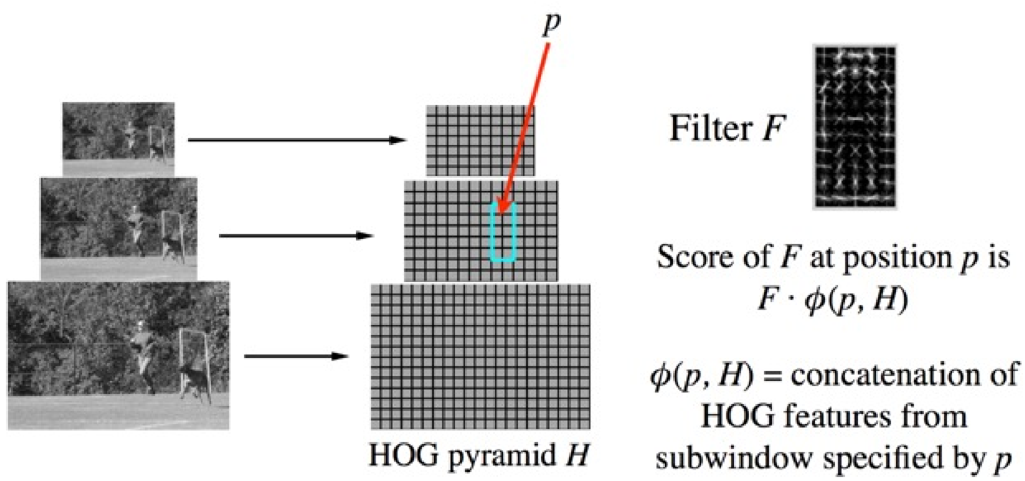

Figure 13: Using a feature pyramid of different image resizings allows the object template to match with objects that might have originally been bigger or much smaller than the the template. Image source: Lecture 15, Slide 40
.

bag of words approach, in which we represent a paragraph as a set of words, or an image as a set of image parts. We can apply a similar idea here and detect an object by its parts instead of detecting the whole singular object. Even if the shape is slightly altered, all of the parts will be present and in approximately the correct position with some minor variance.

5.1 Early Deformation Model for Face Detection

In 1973, Fischler and Elschlager developed a deformable parts model for facial recognition [4]: the parts of the face (such as eyes, nose, and mouth) are detected individually, and there are spring-like connections between each part that allows each part to move slightly, relative to the other parts, but still largely conform to the typical configuration of a face. This allows a face to be detected even if the eyes are farther apart or a change in orientation pushes some parts closer together, since each part has some flexibility in its relative location in the face. See Figure 14 for illustration

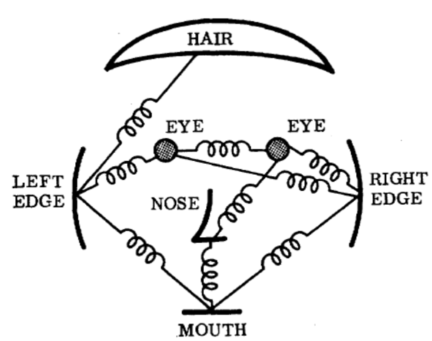

Figure 14: An illustration of Fischler and Elschlager's deformable face model[4]
.

More formally, the springs indicate that there is a desired relative position between two parts, and just like a spring stretches or compresses, we allow some deviations from that desired position, but apply an increasing penalty for larger deviations, much like a string pulls back harder and harder as it is stretched further.

5.2 More General Deformable Parts Models

The deformable model depicted in Figure 14 is one specific deformable model for face detection, where Fischler and Elschlager chose springs between parts that worked well with their methods for face detection. For a more general deformable parts model, one popular approach is the star-shaped model, in which we have some detector as the root and we have springs between every other part and the root (see Figure 15a for illustration)

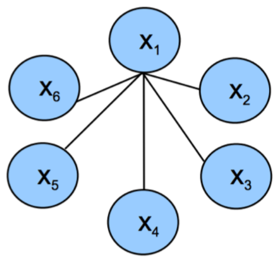

(a)

(b)

Figure 15: On the left is a visualization of the star model, with x1 as the root, and on the right is an example of person detection with a star model for deformations

In face-detection, for example, we could have a detector for the entire body as the root and thus define the location of all body parts relative to the location of entire body. This is shown in Figure 15b, where the cyan box is the location of the bounding box from global person detection (which we use as the root) and the yellow boxes are the bounding boxes resulting from the detection of each part.

This means that the head should be near the top-center of the global location of the person, the feet should be near the bottom, the right arm should be near the left of image (if detector is for a front facing person), etc. In this class we will assume that we already know which parts to use (such as head, arms, and legs if we are detecting people), but it is possible to learn the parts for optimal object detection through machine learning

5.3 Examples of Deformable Parts Models

It is typical to use a global detector for the desired object (such as a person or a bike) as the root, and to use smaller and more detailed filters to detect each part. As a simple example, see Figure 16

It is also common to use a multi-component model for multiple orientations of an object, in which we have a global filter and multiple parts filters for each orientation. A deformable model will protect against the changing positions of parts due to mild rotation, but for more significant rotations such as 90 degrees, all of the parts looks different and require different detectors for each rotation. As an example, in figure 17, each row corresponds to an orientation. Also, the left column is a global car detector for a particular orientation, the middle column contains all of the finer detailed parts filters for that orientation, and the right column shows the deformation penalties for each part in that orientation (where darker grey in the center is smaller penalties and white further from the center is larger penalties).

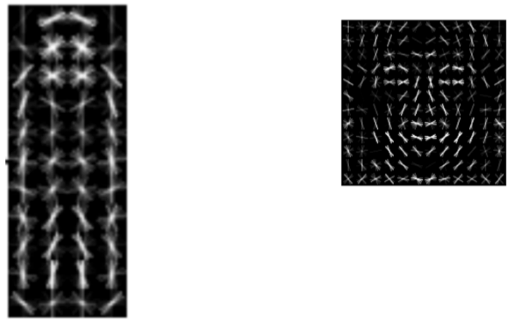

Figure 16: A global HOG filter for a person and a more detailed HOG filter for the head

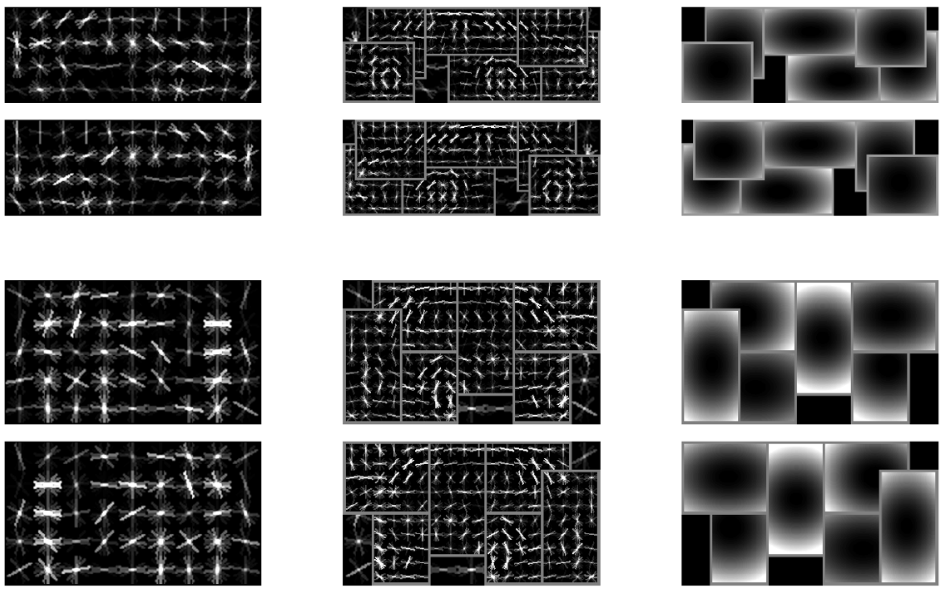

Figure 17: Deformable Parts model of a car with multiple orientations

As another example, consider 2 orientations for bike detection. A bicycle looks very different from the front and from the side so we want multiple detectors. Here we can see the parts identified in the original image alongside the deformable model

5.4 Calculating Score for Deformable Parts Models

To implement a deformable parts model we need a formal way to calculate score. To do this we will calculate a global score from the global object detector, and then calculate a score for each part, determined by it's deformation penalty. The final score is the global score minus all of the deformation penalties, such that an object that is detected strongly but has many of the parts very far from where they should be will be highly penalized.

To express this more formally we will first define some variables: The entire model with n parts is encompassed by an (n+2) tuple:

$$(F_0, P_1, P_2, ...P_n, b)$$

where F_0 is the root filter, P_1 is the model for the first part, and b is a bias term. Breaking it down further, each part's model P_i is defined by a tuple

$$(F_i, v_i, d_i)$$

where F_i is the filter for the i-th part, v_i is the "anchor" position for part i relative to the root position, and d_i defines the deformation cost for each possible placement of the part relative to the anchor

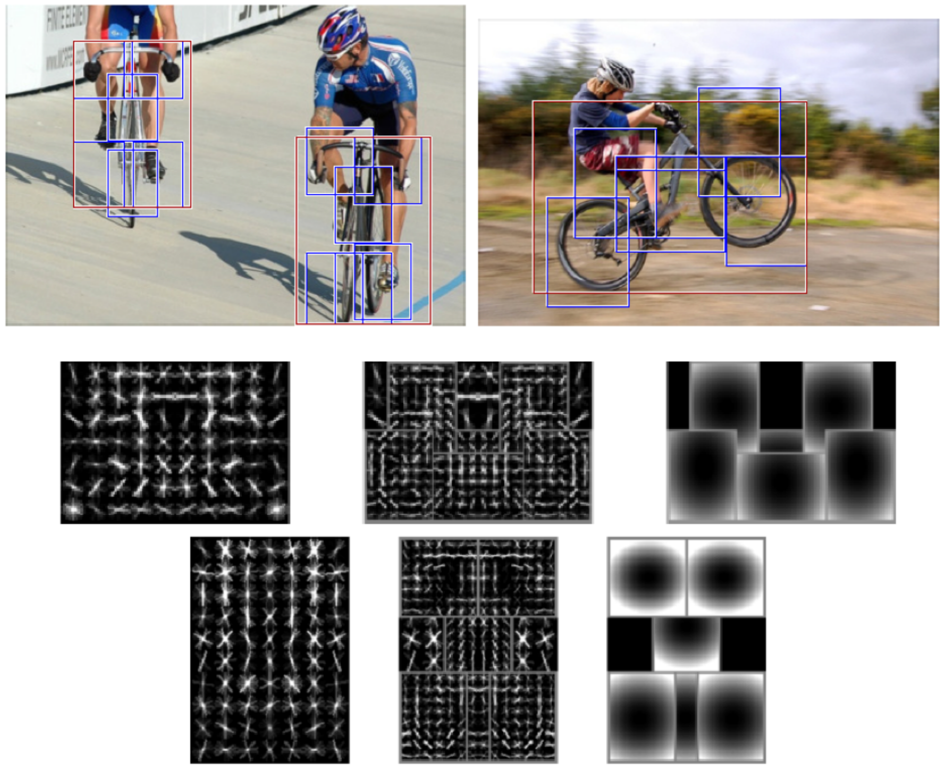

Figure 18: Deformable Parts model of a bike with original image shown

position.

We can calculate the location of the global filter and each part filter with a HOG pyramid (see Figure 19). We run the global HOG filter and each part's HOG filter over the image at multiple scales so that the model is robust to changes in scale. The location of each filter is the location where we see the strongest response. Since we are taking the location of responses across multiple scales we have to take care that our description of the location of each part is scale-invariant (one way this can be done is by scaling the maximum response map for each part up to the original image size and then taking scale-invariant location).

We calculate the detection score as

$$\prod_{i=0}^{n} F_i \cdot \phi(p_i, H) - \sum_{i=1}^{n} d_i(dx_i, dy_i, dx_i^2, dy_i^2)$$

Taken as a whole, this means that we are finding detection score of the global root and all the parts and subtracting all of the deformation penalties.

The left term represents the product of the scores for the global filter and each part filter (note that this is identical to the simpler Dalal and Triggs [1] or sliding window method explained previously). Recall that the score for each filter is the inner product of the filter (as a vector) and $\phi(p_i, H)$ (defined as the HOG feature vector of a window defined by position p_i of the filter). Note that the windows can be visualized in the HOG pyramid in Figure 19: the window for the root is the cyan bounding box, and the window for each of the parts is the yellow bounding box corresponding to that part. We are taking the HOG feature vector of the portion of the image enclosed in these bounding boxes and seeing how well it matches with the HOG features of the template for that part.

$p_i = (x_i, y_i, l_i)$ specifies the level and position of the i-th filter

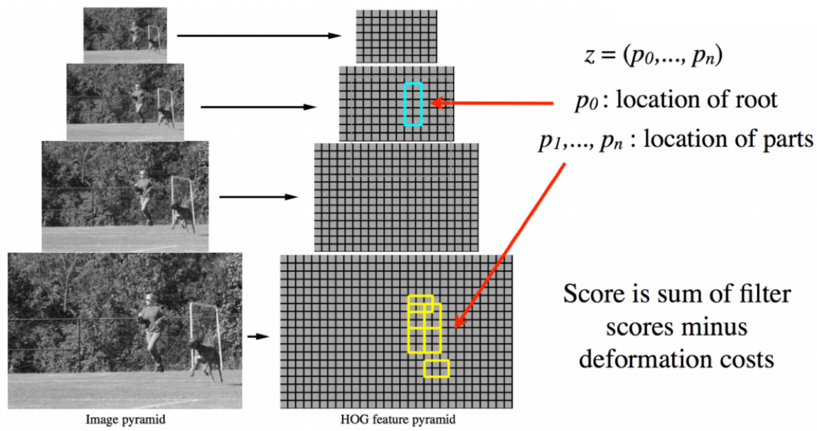

Figure 19: Illustration of HOG pyramid for deformable parts detector

Returning to the score formula, the right term represents the sum of the deformation penalties for each part. We have d_i representing the weights of each penalty for part i, corresponding to quantities dx_i (the distance in x direction from the anchor point where the part should be), dy_i (the distance in y direction from the anchor point where the part should be), as well as dx_i^2 and dy_i^2. As an example, if $d_i = (0, 0, 1, 0)$, then the deformation penalty for part i is the square of the distance in the x direction of that part from the anchor point. All other measures of distance are ignored.

6 The DPM Detection Pipeline

The Deformable Parts Model detection pipeline has several stages. We must first use the global filter to detect an object. Then, the parts filters are used to calculate the overall score of that detection.

1. Generate copies of the original image at different resolutions (so that the fixed window size can capture objects at varied scales); store the HOGs for these different resolutions, as that is what the filters will be applied to.

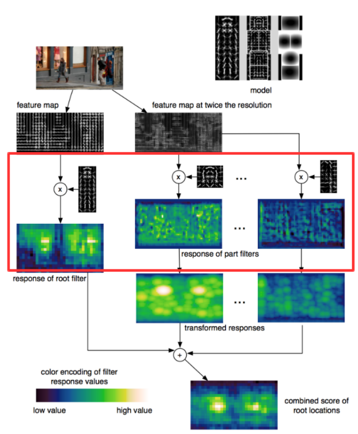

Figure 21: Step 2 of the detection pipeline

2. Apply the global filter to these images. Upon a detection by the global filter, apply the parts filters. This step represents the section of the pipeline depicted in Fig. 21, and contributes the term:

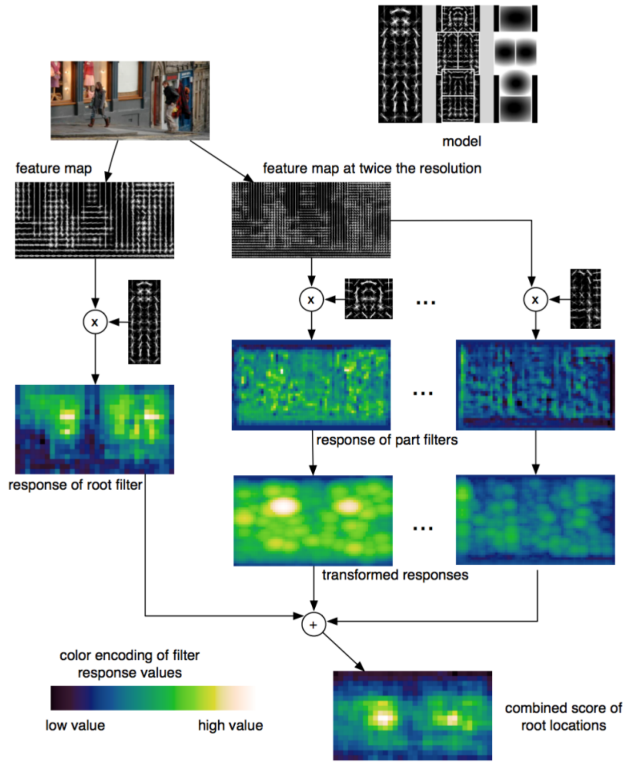

Figure 20: Illustration of full DPM Pipeline

$$\prod_{i=0}^{n} F_i \cdot \phi(p_i, H)$$

3. Having applied the parts filter, we now calculate the spatial costs (i.e., a measure of the deformation of the parts with regards to the global):

$$\sum_{i=1}^{n} d_i(dx_i, dy_i, dx_i^2, dy_i^2)$$

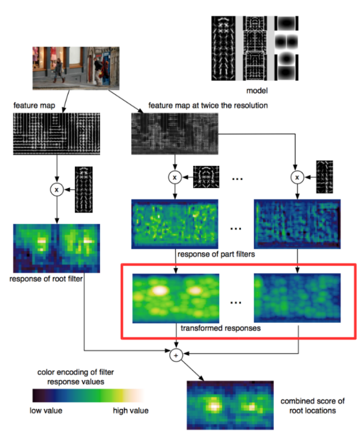

Figure 22: Step 3 of the detection pipeline

4. For every detection, we now sum these components to calculate the *detection score*:

$$F_0 + \prod_{i=1}^{n} F_i \cdot \phi(p_i, H) - \sum_{i=1}^{n} d_i(dx_i, dy_i, dx_i^2, dy_i^2)$$

5. These scores then represent the strength of the detection of the given object at each coordinate of the image; hence, we can plot the response scores throughout the image:

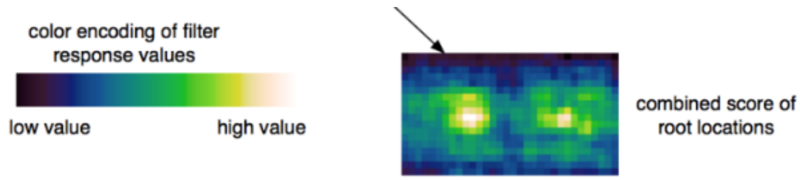

Figure 23: Response scores

7 DPM Detection Results

The Deformable Parts Model makes some key assumptions: an object is defined by a relationship between a global representation (e.g., a car) and representations of parts (e.g. wheels, or a bumper); that the strength of this detection increases with the decrease in deformation between the root and the parts; and that if a high response score is achieved, that object is indeed present (regardless of the potential presence of different categories of objects). Hence, DPM is vulnerable to error in situations where these assumptions are violated:

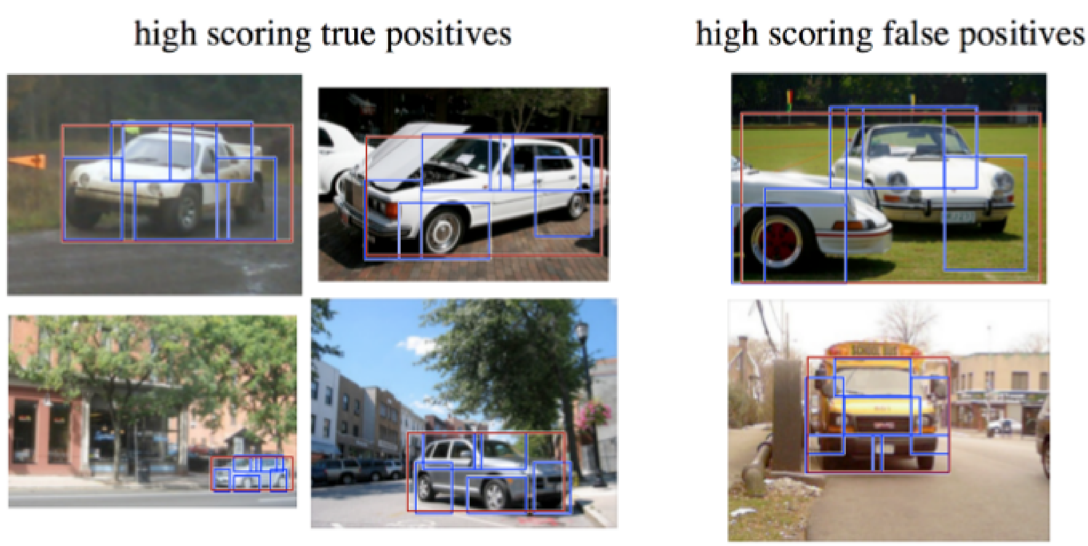

Figure 24: Typical errors for the DPM model

Note how in the top image on the right, DPM has successfully found sections matching the parts filters: wheels and a windshield. DPM has also successfully found one true positive for the global filter (the car in the background). However, DPM assumes that these parts are related to each other because they are spatially close (i.e., they fit the deformation model), and that they correspond to the car identified as the global filter – when in reality, there is not one but two cars in the image providing the parts.

Similarly, with the bottom image, DPM indeed detects an object very close to a car. However, since it does not take into account that the object is even closer to being a bus than a car, and does not take into account features explicitly *not* present in a car (e.g., the raised roof spelling "School bus"), DPM results in a wrong detection.

8 DPM Summary

Approach

- Manually selected set of parts: a specific detector is trained for each part
- Spatial model is trained on the *part* activations
- Joint likelihood is evaluated for these activations

Advantages

- Parts have an intuitive meaning
- Standard detection approaches can be used for each part
- Works well for specific categories

Disadvantages

- Parts need to be selected manually
- Semantically motivated parts sometimes don't have a simple appearance distribution
- No guarantee that some important part hasn't been missed
- When switching to another category, the model has to be rebuilt from scratch

Notably, the Deformable Parts Model was state-of-the-art 3-4 years ago, but has since fallen out of favor. Its "fully-connected" extension, pictured below, is particularly no longer used in practice:

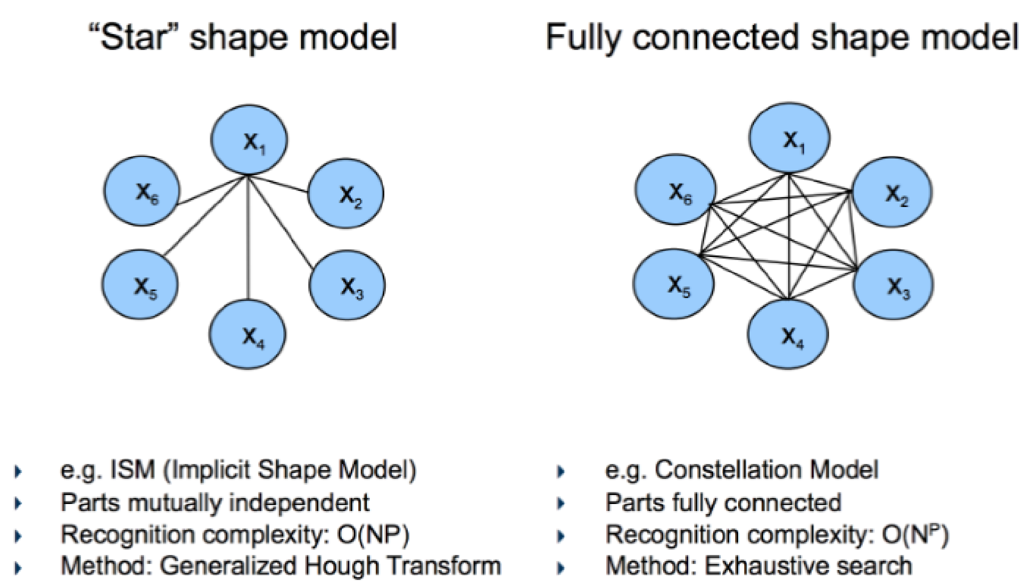

Figure 25: DPM extension: fully-connected shape model

References

[1] Bill Triggs Dalal Navneet. Histograms of oriented gradients for human detection. *Computer Vision and Pattern Recognition, 2005. CVPR 2005. IEEE Computer Society Conference on*, 1, 2005.

[2] M. Everingham, L. Van Gool, C. K. I. Williams, J. Winn, and A. Zisserman. The PASCAL Visual Object Classes Challenge 2012 (VOC2012) Results. http://www.pascal-network.org/challenges/VOC/voc2012/workshop/index.html.

[3] Tsung-Yi Lin, Michael Maire, Serge J. Belongie, Lubomir D. Bourdev, Ross B. Girshick, James Hays, Pietro Perona, Deva Ramanan, Piotr Dollár, and C. Lawrence Zitnick. Microsoft COCO: common objects in context. *CoRR*, abs/1405.0312, 2014.

[4] Robert A. Elshlager Martin A. Fischler. The representation and matching of pictorial structures. *IEEE Transactions on Computers (Volume: C-22, Issue: 1, Jan. 1973)*, 1973.

[5] Olga Russakovsky, Jia Deng, Hao Su, Jonathan Krause, Sanjeev Satheesh, Sean Ma, Zhiheng Huang, Andrej Karpathy, Aditya Khosla, Michael Bernstein, Alexander C. Berg, and Li Fei-Fei. ImageNet Large Scale Visual Recognition Challenge. *International Journal of Computer Vision (IJCV)*, 115(3):211–252, 2015.